Nanoscale

Temperature responsive nanoparticles: Poloxamers as a modulator of Forster resonance energy transfer (FRET).

Journal:	*Nanoscale*
Manuscript ID	NR-ART-02-2018-001278.R1
Article Type:	Paper
Date Submitted by the Author:	30-Mar-2018
Complete List of Authors:	Klep, Oleksandr; Clemson University, Materials Science Bandera, Iurii; Clemson University, Foulger, Stephen; Clemson University, Materials Science

Journal Name

ARTICLE TYPE

Cite this: DOI: 10.1039/xxxxxxxxxx

Temperature responsive nanoparticles: Poloxamers as a modulator of Förster resonance energy transfer (FRET)†

Oleksandr Klep,[a,b] Yuriy Bandera,[a,b] and Stephen H. Foulger[a,b,c]

Received Date
Accepted Date

DOI: 10.1039/xxxxxxxxxx

www.rsc.org/journalname

An effective strategy to control the Förster resonance energy transfer (FRET) of a donor/acceptor emitter pair that were attached to a 60 nm poly(propargyl acrylate)(PA) nanoparticle using temperature variations was developed. The size dependent properties of a poly-(ethylene oxide)-poly-(propylene oxide)-poly-(ethylene oxide) (PEO-PPO-PEO) block copolymer (poloxamer) was exploited to vary the spatial separation of the emitters and vary the FRET efficiency. Specifically, a 2% change in FRET efficiency between the donor/acceptor pair was achieved per 1 °C change in temperature from 49 °C to 60 °C when using a poloxamer of 2950 g/mole molecular weight, with sections of PPO consisting of 32 repeat units, PEO sections consisting of 12 repeat units and a lower critical solution temperature (LCST) of 58 °C. The methodology presented in this effort is easily extended to other temperature regimes through a judicious choice in poloxamer and corresponding LCST. *e.g.* [Surname *et al., Journal Title*, 2000, **35**, 3523].

1 Introduction

A particularly interesting and well-known optical emitter-emitter interaction is Förster resonance energy transfer (FRET) and has been widely utilized as a tool for signaling[1,2] and measuring[3] molecular associations in biomedical and clinical applications, although many applications exploit FRET, including, photovoltaics[4], lighting & displays[5], and sensors[6]. FRET is a near-field nonradiative energy transfer between pairs of dipoles where the excitation energy is transferred from one emitter, referred to as the "donor", to a second emitter, referred to as the "acceptor"**?** .

Extensive research has been done on utilizing organic dyes in FRET assays with much success[7]. These small molecule systems have the advantage of simple preparation and low cost, resulting in a large variety of these dyes being commercially available for diverse applications. Nonetheless, these systems can suffer from poor photo-bleaching resistance[8], short fluorescence life time, low fluorescence quantum yield[9], non-specific quenching[10,11], low chemical stability and intracellular toxicity. In addition, small molecule dyes often will bind to proteins[12], which leads to aggregation and subsequent elimination from the body. In response to the limitations, fluorescent proteins are being used increasingly in FRET systems. In these systems, a fluorophore is genetically appended onto the gene coding for a protein of interest so that a fluorophore and protein can then be co-expressed intracellularly and, when imaged, reveal the location and relative expression level[13,14]. Since the initial development of green fluorescent protein (GFP), efforts on extending the color regime of the protein have resulted in a range of available colors for the fluorescent proteins[15]. Though these systems continue to develop and offer exciting new applications, there are challenges to coupling them to targeting, diagnostic, and therapeutic payloads.

One approach to remedy these shortcomings is the inclusion of the chromophores on the surface of colloidal particles[16–19]. This attachment of the dye to a particle results in an extension of circulation half-life and enhanced *in vivo* stability relative to the free fluoroprobe[18]. The surface attachment of the dyes allows them to participate in advantageous host/guest assemblies that can alter their emission and FRET efficiency. This response can be utilized as a biologically-based sensor or switch due to the noticeable variations in the emission spectra when they form supra-molecular host/guest assemblies or complex with bio-macromolecules[20–24]. The environmental sensitivity in the emission properties of the chromophores can also be exploited to assist in refining the proposed parameters that govern molecular recognition[25–28]. Photo-

[a]*Center for Optical Materials Science and Engineering Technologies (COMSET), Clemson University*
[b]*Clemson University, Department of Materials Science and Engineering, Advanced Materials Research Laboratory 226, Anderson SC USA. Fax: 01 864-656-1049; Tel: 01 864-656-1045; E-mail: foulger@clemson.edu*
[c]*Department of Bioengineering, Clemson University*

† Electronic Supplementary Information (ESI) available: [details of any supplementary information available should be included here]. See DOI: 10.1039/b000000x/

‡ Additional footnotes to the title and authors can be included *e.g.* 'Present address:' or 'These authors contributed equally to this work' as above using the symbols: ‡, §, and ¶. Please place the appropriate symbol next to the author's name and include a `\footnotetext` entry in the the correct place in the list.

stable fluorescence nanoparticles which can be good candidates as donors in FRET that have received recent attention include semiconductor quantum dots (QDs)[29], graphene quantum dots (GQDs)[30,31] and upconversion nanoparticles (UCNPs)[32,33].

In the current effort, colloidal particles are developed that exhibit a significant change in FRET efficiency within a specified temperature regime. The methodology utilized is relatively general, and the system can be easily extended to operate in a wide range of temperature zones. Specifically, sub-100 nm particles are surface modified with two dyes that form a FRET pair. One of the dyes is attached to the particle through a copolymer that exhibits significant changes in its dimensions with temperature variations, and this temperature sensitivity is exploited to alter the spatial proximity of the donor and acceptor dyes, which alters the dyes' FRET efficiency and thus reporting on the temperature alteration. The class of polymer used is a poly(ethylene glycol)-*block*-poly(propylene glycol)-*block*-poly(ethylene glycol) (PEO-PPO-PEO) difunctional block copolymer often referred to as a "poloxamer". Poloxamer copolymers can change their excluded volume ("size") depending on the surrounding temperature and can form hydrophobic pockets that attract hydrophobic molecules, especially aromatic molecules, and stabilize them in aqueous environments[34–36]. This property is utilized in medical applications to promote the activity of hydrophobic dyes and drugs, that are otherwise ineffective in the aqueous environment of live cells[37,38]. Another advantage of using poloxamers comes from their tri-block copolymer structure. The outer blocks are composed of ethylene oxide (EO) which is known to form vesicles that can engulf a payload rendering it invisible to the reticulo-endothelial system and macrophages, and therefore significantly increasing the lifetime of the payload in the body[39–42]. In addition, poloxamer surfactants have been reported to increase the sensitization of tumors with respect to various anticancer agents[43–45], making anticancer drugs more effective.

Unfortunately, free poloxamers cannot create stable polymersomes below critical micellization concentration or temperature and they require additives to make stable vesicles[46] or the attachment to a nanoparticle to create a stable platform[40,42]. Free floating poloxamers are very sensitive to the load that they carry and to the surrounding conditions[35], increasing the likelihood that the formed micelles will be damaged, which results in the loss of content effectively rendering them useless or, worse, triggering an unwanted side effects, such as general system toxicity. Immobilization of the poloxamer on the surface of nanoparticles eliminates these issues allowing the system to maintain its functionality[37]. Based on these characteristics, a poloxamer was chosen as the responsive component of the proposed colloidal device. In addition, the use of a particle as the platform on which various other "loads" can be attached[47,48] is advantageous as it allows for further modifications with targeting ligands and therapeutic drugs[49,50].

2 Results and Discussion

Figure 1A presents the system utilized in this study, which was composed of a propargyl acrylate (PA) nanoparticle, which had two complementary FRET dyes attached to its surface, with the acceptor dye being attached to the particle through a modified poloxamer. The donor dye was an oxadiazole derivative (azOx, cf. Figure 1B) that was attached directly to the surface of the PA nanoparticle through an azide-alkyne Huisgen cycloaddition resulting in a 1,2,3-triazole ("click" transformation)[47], while the acceptor dye, a naphthalimide derivative (azPlurNaph, cf. Figure 1C), was attached to the same nanoparticle through a poloxamer chain. The poloxamer (Pluronic-L64) was a poly(ethylene glycol)-*block*-poly(propylene glycol)-*block*-poly(ethylene glycol) (PEO-PPO-PEO) difunctional block copolymer that initially terminated in primary hydroxyl groups but was modified so that one end contained a naphthalimide dye and the other an azide group so that it could also be "clicked" to the particle (cf. Experimental methods). The unmodified PEO-PPO-PEO triblock copolymer had a molecular weight of 2950 g/mole, with the sections of PPO consisting of 32 repeat units, while the PEO section consisted of 12 repeat units. The poloxamer exhibits a lower critical solution temperature (LCST) of 58 °C.

Free poloxamers typically form polymersomes of several hundred nanometers[35]; however, immobilizing them on nanoparticles of a fixed size limits the maximum size of the system to the sum of the size of the nanoparticle used plus twice the length of the fully extended poloxamer chain. Vesicle size is very important in therapeutic applications due to cell wall permeability limitations. In general anything greater than 200 nm will not be able to enter the cell through a simple diffusion process and anything smaller than 30 nm will be evacuated prematurely through the urinary system[47,51,52]. In this study we used nanoparticles with an average size of 60 nm, and a poloxamer with a theoretical fully extended length of almost 15 nm, which yields a total theoretical maximum size of approximately 90 nm, which is within the desired size range for medical applications.

Figure 2 presents the photoluminescence (PL) at ca. 20 °C in water of the particles with the dual dye-modification (PA/azOx/azPlurNaph) at a grafting density of ca. 0.4 - 0.5 dye molecules per nm^2, as well as two additional sets of nanoparticles with similar grafting densities of dyes; for particles with an emission at 400 nm, the concentration of the particles in water was adjusted to give a comparable emission intensity at this wavelength. One set of the nanoparticles was prepared with azOx and a poloxamer that had not been modified with the naphthalimide dye (PA/azOx/azPlur), while the other set of particles had been modified with only the azPlurNaph dye (PA/azPlurNaph). The poloxamer was attached to the first set of particles to ensure a similar environment for the azOx dye. For the PA/azOx/azPlur, the excitation energy at 335 nm is within the absorbance window of the azOx dye and the particles exhibit an oxadiazole-based emission (cf. Figure 1B) at 400 nm. The excitation wavelength is on the edge of the absorbance window of the naphthalimide dye (cf. Figure 1C) and this, coupled with the aqueous environment of the particles, resulted in the PA/azPlurNaph particles not exhibiting any appreciable emission, though exciting the particles at 400 nm did result in an naphthalimide-based emission (spectra not presented). When excited at 335 nm, the PA/azOx/azPlurNaph particles did exhibit emission characteristics of both the oxadiazole and naphthalimide dyes, indicating that energy transfer is

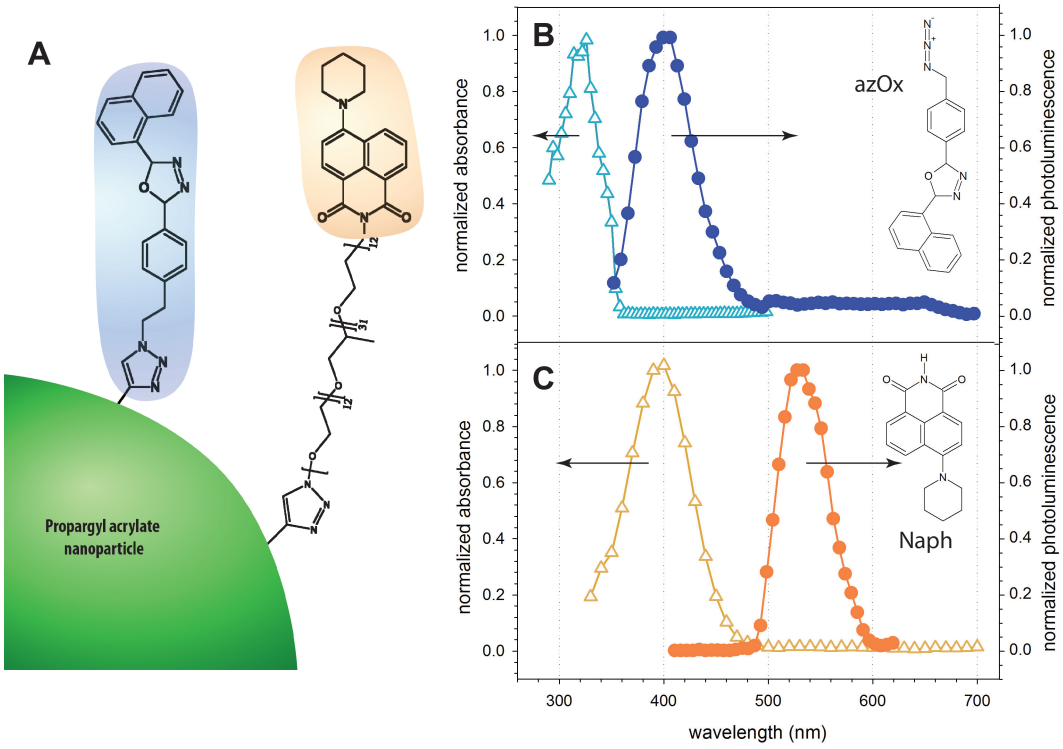

Fig. 1 (**A**) Schematic representation of the built system, showing positioning of the dyes on the surface of the nanoparticle. (**B**) Emission and absorption patterns of donor dye (oxadiazole derivative - azOx) measured in tetrahydrofuran; excitation at 335 nm. (**C**) Emission and absorption patterns of acceptor dye (naphthalimide - Naph) measured in tetrahydrofuran; excitation at 400 nm.

taking place from the azOx to the azPlurNaph dyes, though there is an incomplete transfer since the emission of the oxadiazole-based dye is still present in the spectra.

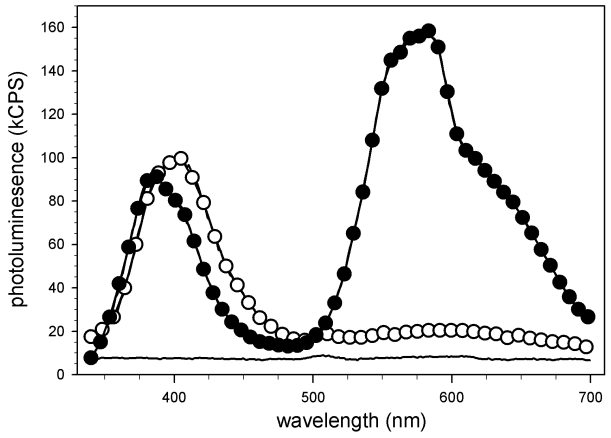

Fig. 2 Photoluminescence of particles: (1) modified with oxadiazole dye (azOx) and poloxamer (○); modified with poloxamer terminated with naphthalimide dye (azPlurNaph) (—); (3) modified with both dyes azOx and azPlurNaph (•). All particles excited at 335 nm. Measurements taken at a temperature of ca. 20 °C in deionized water.

Utilizing FRET theory[?] and the photoluminescence (PL) response of the PA/azOx/azPlurNaph particles (cf. Figure 2-3), the distance and energy transfer efficiency between the dyes were calculated. The FRET efficiency for the system was calculated using the half-lifetimes of the two sets of the nanoparticles. The first set contained the donor dye (azOx) and the poloxamer, the second set contained both the donor dye (azOx) and the acceptor dye (azPlurNaph). By comparing the ratio of the half-lifetime of the donor alone and the half-lifetime of the donor in the presence of the acceptor, the FRET efficiency was calculated[?] . Based on the emission and absorption spectra of azOx and azPlurNaph, the Förster distance was found to be 3.54 nm with a transfer efficiency of ca. 70 % at 20 °C for the given pair of dyes when both of them are attached to the same nanoparticle as shown on Figure 1A.

The component selection of the particles was designed to maximize the FRET efficiency between the fluorophores. To achieve a high level of energy transfer between a pair of dyes, emission of the donor has to have a significant spectral overlap with the absorption of the acceptor[?] . The naphthalimide (azPlurNaph) and oxadiazole (azOx) dyes employed in this effort satisfy this requirement; there is almost 100 % overlap of the donor emission with the absorption of the acceptor (cf. Figures 1B,C). The grafting density was determined to be ca. 0.54 molecules per nm^2 for the donor dye (azOx) and 0.39 molecules per nm^2 for the acceptor dye (azPlurNaph). Since FRET is very sensitive to the distance between dyes, it is expected that by controlling this distance one can achieve control over the extent of FRET[?] .

Poloxamer copolymers are known to change their coil dimen-

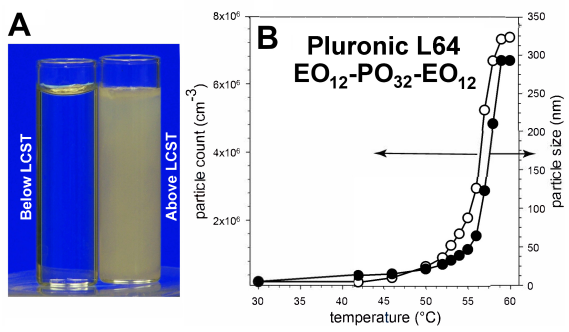

Fig. 3 **(A)** Optical image of neat Pluronic-L64 (poloxamer/water) solution at room temperature (left vial) and at 60 °C (right vial) (LCST is 58 °C). **(B)** Dependence of micelles size and number of micelles formed by Pluronic-L64 in water with solution temperature (measured through dynamic light scattering).

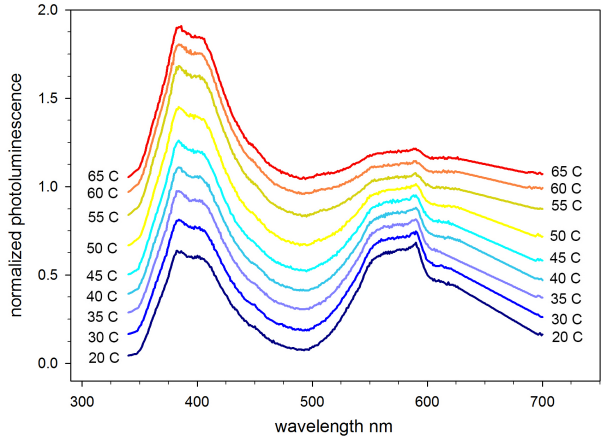

Fig. 4 Photoluminescence spectra of PA/azOx/azPlurNaph particles at various temperatures. The donor dye is azOx with a peak emission ca. 400 nm, while the acceptor dye is azPlurNaph with a peak emission ca. 550 nm. The LCST of the poloxamer, on which the acceptor dye is attached at the end, is 58 °C. Particles dispersed in deionized water and graphs are shifted for clarity. Excitation energy at a wavelength of 335 nm.

sions as a function of temperature, and these changes are reversible and predictable for a given composition of the copolymer[35]. The Pluronic-L64 poloxamer exhibits significant changes in its end-to-end distance with temperature variations and was employed as a means for modulating the distance (and FRET) between the donor/acceptor dyes. In Figure 3A, a neat Pluronic-L64/water solution goes from a transparent solution to a turbid one as the temperature passes through its LCST, while Figure 3B presents the micelles dimensions of the neat Pluronic-L64 poloxamer with temperature variations as analyzed through dynamic light scattering (DLS) procedures[53]. The size of the neat poloxamer appears to exhibit a dramatic increase between 50 °C and 60 °C, going from ca. 50 nm to 300 nm, which coincides with the lower critical solution temperature (LCST) temperature of the polymer (58 °C). In this temperature range, one can expect to see the largest changes in the FRET efficiency of the PA/azOx/azPlurNaph particles to occur. The DLS results are not indicative of the size of the copolymer coils, but are essentially measuring the scattering of the polymer coils as they go from a miscible state (low scattering entity) to a highly scattering dispersion with the increase in temperature.

The photoluminescence dependence on temperature of the PA/azOx/azPlurNaph particles is presented in Figure 4. At 20 °C, the PL response of the particles indicates that both dyes are emitting when excited by a 335 nm excitation, as is expected from the previously presented PL study at 20 °C (cf. Figure 2). This excitation wavelength is within and outside the absorption regime of the azOx dye and azPlurNaph dye, respectively, and should only result in emission from the donor dye. Nonetheless, the emission profile of the particle clearly has the signature of the azPlurNaph dye, suggesting that there is energy transfer taking place from the donor to acceptor dye. Subsequent scans at higher temperatures indicate a diminishing energy transfer until ca. 60 °C where minimal energy transfer is discernible in the spectral response of the particles. The increase in the emission at ca. 400 nm (azOx) and the decrease in the emission at 580 nm (azPlurNaph) is indicative of a reduction in energy transfer from the oxadiazole to the naphthalimide dye. This change is most pronounced within the 50 - 60 °C range and suggests that the separation distance of the two dyes is becoming larger, thereby frustrating FRET[?] . This temperature range is also within the LCST range for the poloxamer. Surprisingly, according to previous studies on poloxamer behavior, it was expected that as the temperature increased, the poloxamer end-to-end distance would decrease, giving rise to a more compact coil packing[35]. This decrease in the size of the copolymer was expected to bring the two dyes closer together, resulting in an increase in the FRET efficiency, which was not observed.

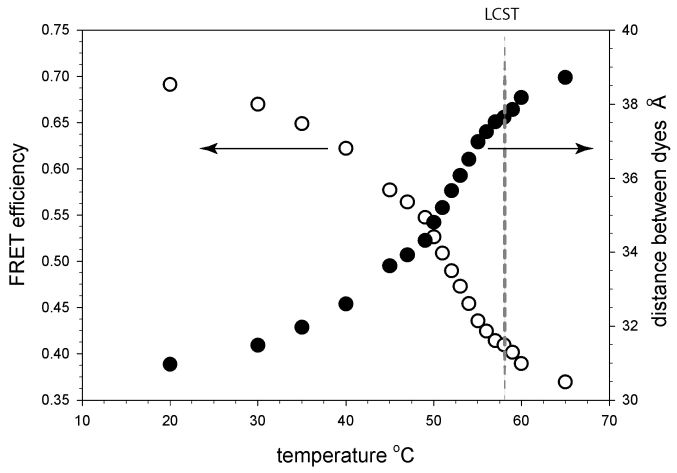

Fig. 5 FRET efficiency (○) and calculated distance between the azOx and azPlurNaph dyes (●) for the PA/azOx/azPlurNaph particles system (in water) presented in Figure 1.

Using the ratio of peak areas for azOx and azPluroNaph dyes at various temperatures referenced to the FRET efficiency at 20°C , the FRET efficiency and corresponding distances between the dyes over a range of temperatures were calculated[?] and are presented in Figure 5. The distance was found to change from 3.1 nm

to 3.9 nm in the 20 °C - 65 °C temperature range, which translates into a change of the FRET efficiency between 70% - 36%. The highest rate of change in the inter-dye distance and corresponding FRET efficiency was observed at temperatures near the LCST temperature of the poloxamer (i.e. 58 °C).

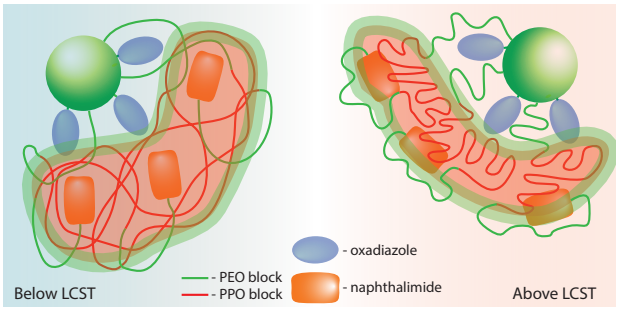

Fig. 6 Proposed mechanism of the variation in photoluminescence response with temperature of PA/azOx/azPlurNaph particles (cf. Figure 1A). At temperatures below LCST, the PPO block forms a hydrophobic domain with loose packing which allows the naphthalimide dye to sequester into its domain, but with a temperature rise above LCST, the PPO domain packs more densely forcing the naphthalimide dye from the domain, resulting in an increase of the distance between donor and acceptor dyes.

We speculate that the simple end-to-end distance argument of the poloxamer to account for FRET efficiency does not account for the poloxamer's unique environment created when it transitions from a coil to an extended structure[34,54]. Previous studies on block copolymer behavior have found that these copolymers can fold their free ends back into the polymer matrix under specific conditions[55]. We speculate that at lower temperatures, the free end of the poloxamer, which contains the hydrophobic naphthalimide dye, folds itself back into the polymer matrix, schematically presented in Figure 6. This folding of the poloxamer brings the two dyes closer together (since the mobility of the oxadiazole dyes is limited), resulting in an enhanced FRET efficiency. As the temperature approaches the LCST of the poloxamer used, packing of the PPO block becomes too dense[35,56,57] and, as a result, the naphthalimide can not fit inside the polymer matrix and is pushed to the outer edge, increasing the distance between the dye and the surface of nanoparticle along with oxadiazole dye, which results in the observed reduced FRET efficiency.

Using the characteristic ratios of ethylene oxide (EO) and propylene oxide (PO) segments of the poloxamer copolymer, the theoretically calculated end-to-end distance of the chain in a theta solvent was calculated to be ca. 4.9 nm[3]. The theta condition is defined as the state when a polymer can not distinguish between itself and its surrounding solvent molecules and adopts relatively "compact" conformations that are defined by local interactions. This calculated value was 58 % to 25 % greater than the shortest and longest, respectively, distance between the dyes obtained from the FRET calculations and supports the concept that the naphthalimide end of the copolymer is folded back into the polymer matrix.

Previous studies have shown that hydrophobic drugs have a tendency to concentrate in the core of a poloxamer PPO block[40,46,58,59]. Additionally, previous reports indicate that hydrophobic drugs sequestered in the PPO domain of a poloxamer can be ejected as the temperature is raised above the LCST of the copolymer[40]. As indicated previously, we speculate for the PA/azOx/azPlurNaph particles at temperatures below the LCST, the PPO block of the poloxamer forms a hydrophobic pocket around the PA particles, which attracts the naphthalimide dye[35], since this layer provides a more favorable condition relative to the aqueous environment outside of these PPO layers (schematically presented on Figure 6). At temperatures higher than the LCST, the packing of the PPO block becomes too dense[38,42,60] to accommodate the naphthalimide dye inside of the layer and the dye is forced out to the outer edge of the polymer matrix, away from the donor dye. This increase in the distance between azOx and azPlurNaph dyes leads to a decrease in the FRET efficiency.

The role of the poloxamer was investigated by modifying a set of particles with a azide fictionalized naphthalimide dye (azNaph) instead of azPlurNaph. These PA/azOx/azNaph particles did not exhibit any emission when dispersed in water and excited at a 335 nm or 400 nm excitation wavelength, indicating that there is fluorescence quenching when the particles do not have the poloxamer on the particles. Dispersing the particles in tetrahydrofuran (THF), a solvent in which both dyes are miscible, resulted in the reappearance of the typical spectra of the dyes. This observation further suggests that changes in the poloxamer state is the main mechanism responsible for the changes in emission patterns for the PA/azOx/azPlurNaph particles when in an aqueous state.

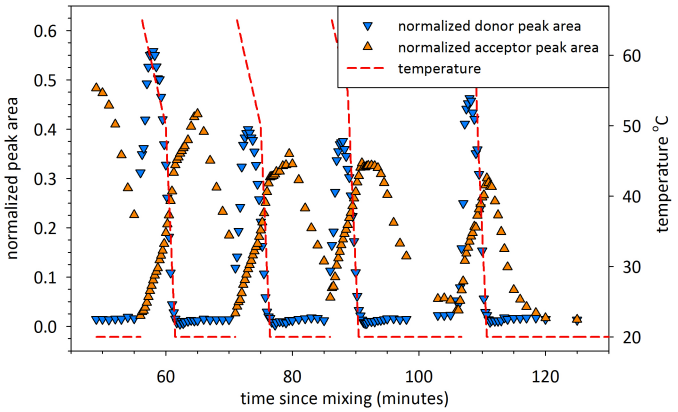

Fig. 7 Normalized integrated emission attributed to azOx (▽) and azPlurNaph (△) dyes in small molecule study performed with azOx, azPlurNaph, and the unmodified poloxamer in deionized water. Sample was repeatedly heated to 65°C (LCST of poloxamer was 58°C) and then allowed to cool down. For the donor dye (azOx), the emission was integrated between 340 nm and 480 nm while for the acceptor dye (azPlurNaph) the emission was integrated between 510 nm and 590 nm. The sample was excited at a wavelength of 335 nm.

To test the proposed mechanism, a small molecule study was performed with just the azOx, azPlurNaph, and the unmodified poloxamer. In this system, the three components were placed in deionized water and excited at a wavelength of 335 nm while the temperature was cycled between 20 °C and 65 °C, all the while observing the emission of the system. The ratio of the dyes was

1 to 1 and total concentration of poloxamer copolymer was 15 mg/ml. The results of the study are depicted in Figure 7, where the integrated emission attributed to the azOx and azPlurNaph dyes is presented relative to time and temperature. Initially at temperatures around 20 °C, there is only an emission from the azPlurNaph dyes (acceptor) that is replaced by an emission from the azOx dye (donor) when the system is heated to 65 °C. We attribute this to the fact that the system initially exhibits FRET between the dyes, at room temperature, and then the energy transfer is disturbed when the system is heated to 65 °C, above LCST of the poloxamer. This emission switching from the azPlurNaph dye to the azOx dye as the temperature is cycled back and forth was repeated multiple times with four cycles being presented in Figure 7.

There is a clear emission switching from the donor dye to the acceptor dye with the temperature cycling. The small molecule model system exhibited the same patterns of emission as the PA/azOx/azPlurNaph particles, but there are two differences. First, the emission of the small molecule system is time dependent (decreases with time) due to the precipitation of the dyes from solution, supporting the need for the particles acting as a stabilizing carrier. Second, the FRET efficiency variation of the small molecule system is much more prominent as compared to the particles. It is hypothesized that almost complete 0 % to 100 % FRET efficiency change exhibited by the small molecule system is due to the much higher mobility of both dyes as compared to the system where the dyes are attached to the nanoparticles. Performing the same study without the poloxamer resulted in no emission since the dyes are hydrophobic and presumably precipitate from solution quickly. Clearly, the poloxamer plays an important role in sequestering the dyes in an aqueous environment, and this role is highly temperature dependent.

3 Conclusion.

In the present work, we achieved control over the changes in FRET efficiency of an emissive colloidal system through the attachment of a donor dye (azOx) directly to the particle surface, while an acceptor dye (azPlurNaph) was attached to the surface of particles through a poloxamer copolymer. The poloxamer (Pluronic-L64) was utilized as the temperature responsive component to regulate the distance between the dyes. The current system achieved its maximum variation in FRET efficiency ($\Delta\varepsilon_{FRET} \approx$20 %) in the temperature range of 49 °C to 60 °C, which is in the region of the cloud point of the poloxamer (LCST) used in this study, though other poloxamers with differing LCST temperatures could be utilized to tune the temperature range of the colloidal device.

4 Experimental methods

4.1 Materials and Reagents

All reagents were purchased from Sigma-Aldrich with at least 97% purity level, while solvents were purified using standard procedures. Oxadiazole-N_3 was synthesized and purified prior to use according to literature procedure[48]; naphthalimide was synthesized prior to use according to literature procedure[61].

4.2 Characterization

^{1}H spectra were recorded on JEOL ECX-300 spectrometers (300MHz for proton). Chemical shifts for protons are reported in parts per million downfield from tetramethylsilane and are referenced to the carbon resonances of the solvent ($CDCl_3$: δ 7.26). Photoluminescence (PL) spectra were collected using Photon Technology International spectrometer equipped with Hamamatsu C9940-01 detector and Jobin-Yvon Fluorolog 3-222 Tau spectrometer. Lifetime measurements were also collected using the Jobin-Yvon Fluorolog 3-222 Tau spectrometer. Nanoparticle size was measured with a Coulter N4Plus DLS using 10 mm quartz cuvettes. UV spectra was obtained using a Perkin Elmer Lambda 850 spectrometer.

4.3 Nanoparticle preparation

Emulsion polymerization was performed in a single necked round bottom flask (50 ml) with magnetic stirring. Potassium persulfate (70 mg) was dissolved in water (29 ml) and nitrogen was purged through the solution for 15 minutes. Sodium dodecyl sulfate solution (29% in H_2O, 0.4 ml) was added to the flask under nitrogen. The resulting solution was stirred and placed in a preheated bath at 70 °C for 3 minutes, then a degassed solution of propargyl acrylate (2 ml) and divinylbenzene (0.1 ml) were added to the main reaction. The mixture was stirred at 70 °C under nitrogen for 90 minutes. The emulsion was cooled, then filtered; followed by purification by dialysis using Spectra/Por Dialysis membrane with MWCO 50000 for 3 days at 40 °C in a dialysis bath, with the water being changed every 8 hours. Nanoparticles were characterized using DLS, median size was 60 nm with a standard deviation of 10 nm. The final emulsion contained 45 mg/ml of nanoparticles.

4.4 Poloxamer modification

$MeSO_2$-pluronic-L64. Pluronic-L64 (3.14 g, 1.064 mmol) was dissolved in dry dichloromethane (DCM) (10 ml), triethylamine (0.132 g, 1.3 mmol) was added to the solution. The obtained solution was stirred at room temperature, and methanesulfonyl chloride (62 mg, 0.543 mmol) was added drop-wise. The mixture was stirred for 6 hours at room temperature; then was washed with water. The organic layer was separated, dried with Na_2SO_4, filtered and evaporated under reduced pressure. Yield 3.1 g (95%), clear oil. This product was used in the next step without further purification. ^{1}H NMR ($CDCl_3$) δ 1.11 (m, 96H), 3.06 (s, 3H), 3.38 (m, 32H), 3.52 (m, 64H), 3.63 (m, 98H).

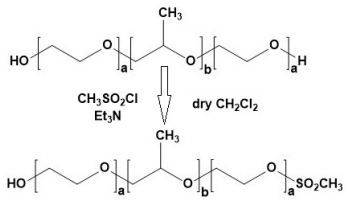

Pluronic-L64-N3. Sodium azide (195 mg, 3 mmol) was added into solution of $MeSO_2$-pluronic-L64 (3.1 g, 1.03 mmol) in dimethylformamide (DMF) (10 ml). The mixture was stirred and

heated to 80 °C for 3 hours. After cooling the mixture was extracted with DCM and washed with water 2 times. The organic layer was separated, dried with Na_2SO_4, filtered and evaporated under reduced pressure. Yield 2.27 g (75%), clear oil. Pluronic-L64-N3 was used in the next step without further purification. ^{1}H NMR ($CDCl_3$) δ 1.07 (m, 96H), 3.34 (m, 32H), 3.48 (m, 64H), 3.59 (m, 98H).

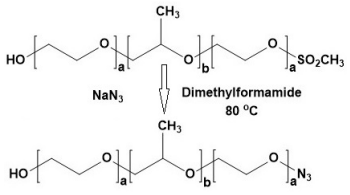

$MeSO_2$-pluronic-L64-N3. Pluronic-L64-N3 (1 g, 0.34 mmol) was dissolved in dry DCM (3 ml), then triethylamine (42 mg, 0.408 mmol) was added. The solution was stirred at room temperature and methanesulfonyl chloride (78 mg, 0.68 mmol) was added drop-wise. The reaction was stirred at room temperature for 6 hours, followed by extraction with DCM and washed with water. The organic layer was separated, dried with Na_2SO_4, filtered and evaporated under reduced pressure. Yield 0.7 g (65%), clear oil. This product was used in the next step without further purification. ^{1}H NMR ($CDCl_3$) δ 1.11 (m, 96H), 3.07 (m, 3H), 3.38 (m, 32H), 3.52 (m, 64H), 3.64 (m, 98H).

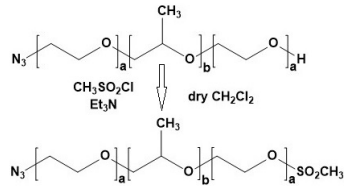

azPlurNaph. The mixture of $MeSO_2$-pluronic-L64-N3 (0.7 g, 0.22 mmol), naphthalimide (100 mg, 0.36 mmol) and potassium carbonate (80 mg, 0.58 mmol) in acetone (15 ml) was stirred and refluxed for 48 hours. The mixture was filtered, and the filtrate was evaporated under reduced pressure; the residue was extracted with DCM and washed with water. The organic layer was separated, dried with Na_2SO_4, filtered and evaporated under reduced pressure. Yield 0.58 g (80%), yellow oil. ^{1}H NMR ($CDCl_3$) δ 1.11 (m, 96H), 1.70 (m, 6H), 1.86 (m, 10H), 3.38 (m, 32H), 3.52 (m, 64H), 3.62 (m, 98H), 7.14 (m, 2H), 7.65 (m, 2H), 8.31-8.54 (m, 8H).

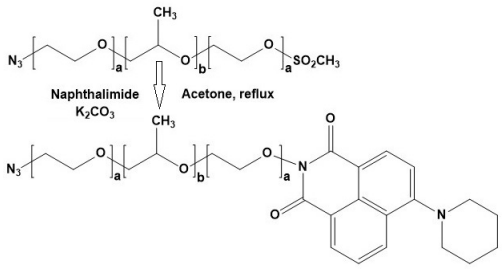

4.5 Nanoparticle modification

Nanoparticle modification was performed using the azide alkyne Huisgen cycloaddition reaction (click chemistry). A typical procedure was used as described elsewhere[48]. In short, copper(II) sulfate ($CuSO_4$) (2 mg, 8 μmol) was added to the propargyl acrylate nanoparticles suspension in water (2 ml) and stirred until completely dissolved. The solution of azOx (2 mg, 7 μmol) in the mixture of tetrahydrofuran (THF) (2 ml) and methanol (4 ml) was added to the suspension of nanoparticles. The stirred reaction vessel was purged with nitrogen for 5 minutes, then sodium ascorbate (10 mg, 50.5 μmol) was added. The mixture was stirred at 28°C for 24 hours under nitrogen; then the solution of azPlurNaph (22 mg, 7 μmol) in THF (2 ml) was added. Then the solution of $CuSO_4$ (2 mg, 8 μmol) in water (2 ml) was added. The reaction was stirred and purged with nitrogen for 5 minutes, then sodium ascorbate (10 mg, 50.5 μmol) was added. The reaction continued at 28 °C for 24 hours under nitrogen. The reaction mixture was centrifuged at 10000G for 5 minutes. Separated nanoparticles were washed with the mixture of THF:Methanol 1:1 (20 ml); this purification was performed 5 times until all impurities were removed. The content of unreacted dyes in the supernatant solution was monitored by observation of UV-Vis absorption (for azOx peak at 330 nm was monitored, for azPlurNaph peak at 400 nm was monitored). When these peaks were impossible to identify the cleaning process was considered complete. After the last centrifugation the nanoparticles were suspended in THF (1 ml) and stored in dark until further use. To prepare single dye modified nanoparticles reagents ratio was calculated based on the sum of the grafting densities of both dyes on dual modified nanoparticles. This was done to match the total number of chromophores per nanoparticle in all sample. The rest of the synthesis procedure was the same as for dual modified nanoparticles.

4.6 Grafting density determination

To determine grafting density of the dyes all supernatant solutions from nanoparticle cleaning process were collected and the dye content in them was calculated using the Beer-Lambert law based on the specific absorption of each dye. The mass of both dyes in all supernatant solutions was calculated and summed. This sum was subtracted from the loading quantities of the dyes to calculate mass of the dyes that had reacted. Total surface area of the nanoparticles was calculated using the assumption that nanoparticles are perfect mono-disperse spheres with 60 nm diameter. The final grafting density for oxadiazole was measured to be 0.54 molecules per nm^2, naphthalimide-pluronic-L64-N3 complex 0.39 molecules per nm^2.

4.7 Fluorescence measurements

Sample preparation procedures for the dual dye-modified nanoparticles fluorescence measurements were as follows: a portion of the particle suspension obtained after cleaning of the modified nanoparticles was dispersed in water to achieve a nanoparticle density of $5x10^{11}$ (checked by DLS), which translates to approximately $5x10^{-9}$ mole/ml of dye. For the single dye-modified nanoparticles, the samples were diluted to achieve a particle den-

sity that gave a PA/azOx peak intensity similar to the dual dye-modified nanoparticles. All samples were allowed 24 hours for equilibration at room temperature prior to any measurement.

Acknowledgements

The authors thank the Gregg-Graniteville Foundation and the National Science Foundation (DMR-1507266) for financial support.

Notes and references

1 B. Schuler, E. A. Lipman and W. A. Eaton, *Nature*, 2002, **419**, 743–747.

2 P. Carriba, G. Navarro, F. Ciruela, S. Ferre, V. Casado, L. Agnati, A. Cortes, J. Mallol, K. Fuxe, E. I. Canela, C. Lluis and R. Franco, *Nature Methods*, 2008, **5**, 727–733.

3 L. Stryer, *Annual Review of Biochemistry*, 1978, **47**, 819–846.

4 S. Buhbut, S. Itzhakov, E. Tauber, M. Shalom, I. Hod, T. Geiger, Y. Garini, D. Oron and A. Zaban, *Acs Nano*, 2010, **4**, 1293–1298.

5 V. Vohra, G. Calzaferri, S. Destri, M. Pasini, W. Porzio and C. Botta, *Acs Nano*, 2010, **4**, 1409–1416.

6 I. L. Medintz, A. R. Clapp, H. Mattoussi, E. R. Goldman, B. Fisher and J. M. Mauro, *Nature Materials*, 2003, **2**, 630–638.

7 K. E. Sapsford, L. Berti and I. L. Medintz, *Angewandte Chemie-International Edition*, 2006, **45**, 4562–4588.

8 F. Pinaud, R. Millereux, P. Vialar-Trarieux, B. Catargi, S. Pinet, I. Gosse, N. Sojic and V. Ravaine, *Journal of Physical Chemistry B*, 2015, **119**, 12954–12961.

9 T. Desmettre, J. M. Devoisselle and S. Mordon, *Survey of Ophthalmology*, 2000, **45**, 15–27.

10 R. Philip, A. Penzkofer, W. Baumler, R. M. Szeimies and C. Abels, *Journal of Photochemistry and Photobiology A-Chemistry*, 1996, **96**, 137–148.

11 S. A. Soper and Q. L. Mattingly, *Journal of the American Chemical Society*, 1994, **116**, 3744–3752.

12 T. J. Muckle, *Biochemical Medicine*, 1976, **15**, 17–21.

13 M. Chalfie, Y. Tu, G. Euskirchen, W. W. Ward and D. C. Prasher, *Science*, 1994, **263**, 802–805.

14 R. Y. Tsien, *Annual Review of Biochemistry*, 1998, **67**, 509–544.

15 N. C. Shaner, P. A. Steinbach and R. Y. Tsien, *Nature Methods*, 2005, **2**, 905–909.

16 P. Rungta, Y. P. Bandera, V. Tsyalkovsky and S. H. Foulger, *Soft Matter*, 2010, **6**, 6083–6095.

17 P. Sharma, S. Brown, G. Walter, S. Santra and B. Moudgil, *Advances in Colloid and Interface Science*, 2006, **123**, 471–485.

18 S. Jin and K. M. Ye, *Biotechnology Progress*, 2007, **23**, 32–41.

19 J. Yu, M. A. Yaseen, B. Anvari and M. S. Wong, *Chemistry of Materials*, 2007, **19**, 1277–1284.

20 M. A. Daniele, M. L. Shaughnessy, R. Roeder, A. Childress, Y. P. Bandera and S. Foulger, *Acs Nano*, 2013, **7**, 203–213.

21 P. Rungta, Y. P. Bandera, M. G. Sehorn and S. H. Foulger, *Macromolecular Bioscience*, 2011, **11**, 927–937.

22 A. C. Bhasikuttan, J. Mohanty, W. M. Nau and H. Pal, *Angewandte Chemie-International Edition*, 2007, **46**, 4120–4122.

23 R. Zadmard and T. Schrader, *Journal of the American Chemical Society*, 2005, **127**, 904–915.

24 R. Jenkins, M. K. Burdette and S. H. Foulger, *Rsc Advances*, 2016, **6**, 65459–65474.

25 M. A. Daniele, Y. P. Bandera, D. Sharma, P. Rungta, R. Roeder, M. G. Sehorn and S. H. Foulger, *Small*, 2012, **8**, 2083–2090.

26 J. R. Babendure, S. R. Adams and R. Y. Tsien, *Journal of the American Chemical Society*, 2003, **125**, 14716–14717.

27 V. S. Jisha, K. T. Arun, M. Hariharan and D. Ramaiah, *Journal of Physical Chemistry B*, 2010, **114**, 5912–5919.

28 V. S. Jisha, K. T. Arun, M. Hariharan and D. Ramaiah, *Journal of the American Chemical Society*, 2006, **128**, 6024–6025.

29 A. P. Alivisatos, W. W. Gu and C. Larabell, in *Quantum dots as cellular probes*, Annual Reviews, Palo Alto, 2005, vol. 7, pp. 55–76.

30 S. N. Baker and G. A. Baker, *Angewandte Chemie-International Edition*, 2010, **49**, 6726–6744.

31 K. P. Loh, Q. L. Bao, G. Eda and M. Chhowalla, *Nature Chemistry*, 2010, **2**, 1015–1024.

32 X. Q. Ge, L. N. Sun, L. Y. Shi and R. Y. Wei, *Biomedical Spectroscopy and Imaging*, 2015, **4**, 391–412.

33 V. Muhr, S. Wilhelm, T. Hirsch and O. S. Wolfbeis, *Accounts of Chemical Research*, 2014, **47**, 3481–3493.

34 D. A. Chiappetta and A. Sosnik, *European Journal of Pharmaceutics and Biopharmaceutics*, 2007, **66**, 303–317.

35 P. Alexandridis, J. F. Holzwarth and T. A. Hatton, *Macromolecules*, 1994, **27**, 2414–2425.

36 G. Bonacucina, M. Cespi, G. Mencarelli, G. Giorgioni and G. F. Palmieri, *Polymers*, 2011, **3**, 779–811.

37 A. V. Kabanov, E. V. Batrakova and V. Y. Alakhov, *Journal of Controlled Release*, 2002, **82**, 189–212.

38 B. Foster, T. Cosgrove and B. Hammouda, *Langmuir*, 2009, **25**, 6760–6766.

39 X. M. Li, L. Y. Ding, Y. L. Xu, Y. L. Wang and Q. N. Ping, *International Journal of Pharmaceutics*, 2009, **373**, 116–123.

40 R. Basak and R. Bandyopadhyay, *Langmuir*, 2013, **29**, 4350–4356.

41 D. E. Discher, V. Ortiz, G. Srinivas, M. L. Klein, Y. Kim, D. Christian, S. Cai, P. Photos and F. Ahmed, *Progress in Polymer Science*, 2007, **32**, 838–857.

42 M. Chiper, K. H. Aubert, A. Auge, J. F. Fouquenet, M. Souce and I. Chourpa, *Nanotechnology*, 2013, **24**, 605–616.

43 V. Alakhov, E. Klinski, S. M. Li, G. Pietrzynski, A. Venne, E. Batrakova, T. Bronitch and A. Kabanov, *Colloids and Surfaces B-Biointerfaces*, 1999, **16**, 113–134.

44 V. Y. Erukova, O. O. Krylova, Y. N. Antonenko and N. S. Melik-Nubarov, *Biochimica Et Biophysica Acta-Biomembranes*, 2000, **1468**, 73–86.

45 A. V. Kabanov, E. V. Batrakova and V. Y. Alakhov, *Advanced Drug Delivery Reviews*, 2002, **54**, 759–779.

46 L. Tavano, R. Muzzalupo, L. Mauro, M. Pellegrino, S. Ando and N. Picci, *Langmuir*, 2013, **29**, 12638–12646.

47 P. Rungta, Y. P. Bandera, R. D. Roeder, Y. C. Li, W. S. Bald-

win, D. Sharma, M. G. Sehorn, I. Luzinov and S. H. Foulger, *Macromolecular Bioscience*, 2011, **11**, 927–937.

48 P. Rungta, Y. P. Bandera, V. Tsyalkovsky and S. H. Foulger, *Soft Matter*, 2010, **6**, 6083–6095.

49 F. Alexis, E. Pridgen, L. K. Molnar and O. C. Farokhzad, *Molecular Pharmaceutics*, 2008, **5**, 505–515.

50 F. Alexis, J. W. Rhee, J. P. Richie, A. F. Radovic-Moreno, R. Langer and O. C. Farokhzad, *Urologic Oncology-Seminars and Original Investigations*, 2008, **26**, 74–85.

51 W. H. De Jong, W. I. Hagens, P. Krystek, M. C. Burger, A. Sips and R. E. Geertsma, *Biomaterials*, 2008, **29**, 1912–1919.

52 P. Jani, G. W. Halbert, J. Langridge and A. T. Florence, *Journal of Pharmacy and Pharmacology*, 1990, **42**, 821–826.

53 L. Sperling, *Introduction to Physical Polymer Science*, 2006, **4th edition**, 845.

54 P. Alexandridis and T. A. Hatton, *Colloids and Surfaces a-Physicochemical and Engineering Aspects*, 1995, **96**, 1–46.

55 E. G. Kelley, J. N. L. Albert, M. O. Sullivan and T. H. Epps, *Chemical Society Reviews*, 2013, **42**, 7057–7071.

56 A. G. Denkova, E. Mendes and M. O. Coppens, *Soft Matter*, 2010, **6**, 2351–2357.

57 G. Fleischer, *Journal of Physical Chemistry*, 1993, **97**, 517–521.

58 I. R. Schmolka, in *Physical basis for poloxamer interactions*, ed. R. C. Lee, M. CapelliSchellpfeffer and K. M. Kelley, New York Acad Sciences, New York, 1994, vol. 720, pp. 92–97.

59 R. Muzzalupo, L. Tavano, S. Trombino, R. Cassano, N. Picci and C. La Mesa, *Colloids and Surfaces B-Biointerfaces*, 2008, **64**, 200–207.

60 B. Sahoo, K. S. P. Devi, R. Banerjee, T. K. Maiti, P. Pramanik and D. Dhara, *Acs Applied Materials & Interfaces*, 2013, **5**, 3884–3893.

61 J. Ren, X. L. Zhao, Q. C. Wang, C. F. Ku, D. H. Qu, C. P. Chang and H. Tian, *Dyes and Pigments*, 2005, **64**, 179–186.

Poloxamer attached to propargyl acrylate nanoparticle is used to control energy transfer between the dyes through distance modulation.